Published in final edited form as:
J Mol Cell Cardiol. 2012 December ; 53(6): 809–819. doi:10.1016/j.yjmcc.2012.08.022.

EBP50 Promotes Focal Adhesion Turnover and Vascular Smooth Muscle Cells Migration

Gyun Jee Song, **Kristen L. Leslie**, **Stacey Barrick**, **Sylvain Bougoin**, **Juan M. Taboas**, and **Alessandro Bisello**
Department of Pharmacology and Chemical Biology (GJS, KLL, SB, AB) and Vascular Medicine Institute (AB), University of Pittsburgh School of Medicine, Center for Craniofacial Regeneration, Department of Oral Biology (SyB, JMT), University of Pittsburgh School of Dental Medicine, Pittsburgh, PA, 15261

Abstract

The Ezrin-Radixin-Moesin-Binding Phosphoprotein 50 (EBP50) is a PDZ-containing scaffolding protein that regulates a variety of physiological functions. In the vasculature, EBP50 promotes neointima formation following arterial injury. In this study the role of EBP50 on vascular smooth muscle cell (VSMC) migration was characterized. The spreading and motility of primary VSMC isolated from EBP50 knockout (KO) mice were significantly reduced compared to wild type (WT) cells. EBP50-null VSMC had fewer and larger focal adhesions than wild type cells. Assembly and disassembly of focal adhesion - assessed by live-cell total internal reflection fluorescence imaging - in response to epidermal growth factor (EGF) were significantly reduced in KO cells. Immunoprecipitation experiments showed that EBP50 interacts with EGF receptor via the PDZ2 domain and with focal adhesion kinase (FAK) via the C-terminal ERM domain. EBP50 promoted the formation of a complex containing both EGF receptor and FAK. Phosphorylation of Tyr-925 of FAK in response to EGF was significantly reduced in KO cell compared to WT cells. The residence time of FAK in focal adhesions - determined by fluorescence recovery after photobleaching - was increased in WT cells. Collectively, these studies indicate that EBP50, by scaffolding EGF receptor and FAK, facilitates activation of FAK, focal adhesion turnover, and migration of VSMC.

Keywords

EBP50; NHERF; FAK; EGF; vascular smooth muscle cell; migration; focal adhesion

Corresponding Authors: Gyun Jee Song, Department of Pharmacology and Chemical Biology, University of Pittsburgh School of Medicine, W1313 Biomedical Science Tower, 200 Lothrop Street, Pittsburgh PA 15261, USA. Tel: 412-648-8132 Fax: 412-648-2229 gys2@pitt.edu. Alessandro Bisello, Department of Pharmacology and Chemical Biology, University of Pittsburgh School of Medicine, E1358 Biomedical Science Tower, 200 Lothrop Street, Pittsburgh PA 15261, USA. Tel: 412-648-7347 Fax: 412-648-2229 alb138@pitt.edu.

Disclosures
None

1. Introduction

Cell migration is a fundamental cellular process that is important during morphogenesis and tissue regeneration and repair [1, 2]. However, unregulated cell migration is a major factor in tumor progression and metastasis [3, 4], and in a number of vascular pathologies [5, 6]. Focal adhesions (FAs) are the cellular microdomains that mediate cell migration [7]. The coordinated formation of FAs at the leading edge and the disassembly of FAs at the trailing edge of a migrating cell provide the directional force for movement [8, 9]. Up to one hundred signaling and structural molecules within FAs regulate this dynamic turnover in response to biochemical signals originating from membrane receptors [10]. Among these, the non-receptor tyrosine kinase focal adhesion kinase (FAK) plays a central role in regulating FA dynamic and cell motility [11, 12]. Numerous studies using FAK-null cells and overexpression of wild type and dominant negative FAK have demonstrated the essential role of this protein in cell migration [13–15]. In addition, evidence for the importance of tyrosine phosphorylation of FAK in regulating its function has emerged. Tyr-397 is an essential site that is auto-phosphorylated upon integrin engagement [16]. Following Tyr-397 phosphorylation, src family kinases phosphorylate other residues (407, 576, 577, 861 and 925) in a cell-type dependent manner [17, 18]. In particular, Tyr-925 phosphorylation has been shown to promote FAK residence time in FAs, FA turnover and cell migration in fibroblasts [19].

The Ezrin-Radixin-Moesin-Binding Phosphoprotein 50 (EBP50), also known as Na^+/H^+ exchanger regulatory factor 1 (NHERF1), is a PDZ domain-containing scaffolding protein [20]. EBP50 was originally identified as a critical regulator of Na^+/H^+ exchanger 3 in the kidney [21]. In addition to the well established regulation of ion homeostasis in the kidney and intestine [22–24], EBP50 exerts important actions on liver biology [25, 26] as well as type-specific contributions to growth and metastatic potential of various cancers, including breast, liver, intestine and brain tumors [27–30].

Recently, significant actions of EBP50 in the vasculature have emerged. EBP50 depletion potentiates the contractile response of mesenteric arteries to noradrenaline [31]. Our studies showed that EBP50 expression increases in arteries following endoluminal denudation and contributes to neointima formation by positively regulating vascular smooth muscle cell proliferation [32, 33]. However, the remarkable inhibition of neointimal hyperplasia in EBP50-null mice suggests that other cellular responses may be affected by EBP50. Of these, VSMC migration is of particular interest because the acquisition of motility is one of the principal phenotypic changes associated with vascular remodeling and the response of VSMC to growth factors and cytokines [5].

Because of the fundamental role of FAs on cell motility and the importance of FAK function in regulating FA dynamics we sought to determine the effect of EBP50 on these processes. To this end we used a combination of biophysical and biochemical approaches to establish the effect of EBP50 on FAK activity and growth factors-induced VSMC migration.

2. Materials and Methods

2.1 Plasmids and Mutagenesis

The plasmid encoding N-terminal Flag-human EBP50 was a gift from Dr. Peter Friedman (University of Pittsburgh). The mutants S1, S2, ΔERM and S1/S2 EBP50 mutant constructs were made from Flag-EBP50 by using the QuikChange site-directed mutagenesis kit from Stratagene (La Jolla, CA). Mutagenic primers were designed based on human EBP50 sequence (S1 mutant, 5’-AGGGTCCGAACGGCGCCGGCGCCCACCTGCACGGGG-3’; S2 mutant, 5’-

GAAGAAGGGCCCCAGTGGCGCTGGCGCCAACCTGCACAGCGACAAGTC-3'; delta ERM, 5'-GACTTCAACATCTCCATGAGCGCGGACGCA-3'). S1/S2 mutagenesis was done by two consecutive mutagenic reactions using S1 and S2 mutagenic primers. DNA sequences were confirmed by sequence analysis (GeneWiz).

2.2 Primary VSMC culture and transfection

All animal experiments were approved by the University of Pittsburgh Institutional Animal Care and Use Committee. Primary VSMC were isolated from abdominal aortic explants from wild type (WT) C57BL/6 and EBP50 knockout (KO) littermate mice and cultured in Dulbecco's modified eagle media (DMEM) containing 10% fetal bovine serum (FBS) in 5% CO_2 at 37°C. All experiments were performed with cells between passages 3 and 15. CHO cells were cultured in Ham's F-12 medium supplemented with 10% FBS. For transient EBP50 expression, EBP50 plasmid was introduced in primary VSMC by electroporation using an AMAXA electroporator and the Basic Nucleofect kit (Lonza). For GFP-tagged FAK expression, primary VSMC were infected with an adenovirus encoding GFP-FAK (a generous gift from Dr. Harold Singer, Albany Medical College, NY). Cells were incubated with adenovirus in serum free media for 1 hour and incubated with 10% FBS-supplemented media overnight. Experiments were performed at 24 hours after infection. CHO cells were transfected using Lipofectamine 2000 (Invitrogen). Transfections with siEBP50 and infections with lentiviral shEBP50 were performed as described previously [33]. Cells were used after 3 days of infection.

2.3 Cell migration assays

Cell migration was analyzed by a scratch wound assay. Cells were grown to confluence in 12 well plates. A scratch wound in the monolayer was performed by dragging a pipette tip across the layer. Detached cells were washed away with PBS. The remaining cells were culture in 10% FBS DMEM or treated as described after 24 hours in 0.1% FBS. The closure of the wound over time was monitored by light microscopy (Olympus IX71). To measure the velocity of cell migration, VSMC were monitored for up to 24 hours on a Nikon TE2000 inverted microscope equipped with a motorized stage and a LiveCell stage incubator system (Pathology Devices, Inc.) that provides temperature, humidity and CO_2 control. Images were captured every 20 min using a x10 objective and a Nikon DS-Fi1 CCD camera controlled by NIS Elements software (Nikon). Moving distances of single cells over time were measured using Image J software (National Institutes of Health). Boyden chamber migration assays were performed using 24-well transwell chambers (BD bioCoat) with a pore size of 8 μm. The upper compartment was filled with 300 μl of a cell suspension containing 5×10^4 cells. Bottom wells were filled with 500 μl of basal medium (DMEM containing 0.5% FBS) without or with growth factors (EGF 10 ng/ml or PDGF 10 ng/ml). Cells were then allowed to migrate for 5 h at 37 °C. Cells were removed from the upper surface with cotton swabs, and the filters were washed in PBS. Cells were fixed in 4% paraformaldehyde in PBS, and stained with 0.1% crystal violet. Images were acquired on a Olympus IX71 microscope using a 20× objective.

2.4 Immunofluorescence analysis

Cells on glass coverslips were fixed with 4% paraformaldehyde and incubated with blocking buffer containing 5% goat serum and 0.2% Nonidet P-40 (NP-40) in PBS. Primary rabbit anti-FAK, anti-paxillin (both Santa Cruz, 1:500), anti-phospho paxillin, vinculin (both Sigma, 1:500) antibodies or phalloidin-red (Cell signaling, 1:2000) were applied in the same buffer overnight at 4 °C. Coverslips were washed with PBS, incubated with Alexa546-conjugated anti-rabbit secondary antibody (1:1000, Molecular Probes) and 4',6-diamidino-2-phenylindole (DAPI, 0.1 μg/ml; Sigma) for 2 h and washed again. Coverslips were mounted for immunofluorescence microscopy and analyzed with an Olympus

Fluoview confocal laser-scanning microscope with a x63 oil immersion objective. The fraction of phospho-paxillin that co-localizes with vinculin (Mander's coefficient) was calculated with the JACoP plug-in for Image J [34].

2.5 Live cell imaging

Total internal reflection fluorescence (TIRF) images were acquired using a Nikon Ti-TIRF microscope equipped with 60x Oil TIRF objective (NA=1.49). VSMC infected with adenovirus encoding GFP-FAK were imaged every minute for 60 min. The fluorescence intensity, the number and the size of focal adhesions of each image were determined with Image J software (National Institutes of Health). Assembly of FAs was calculated by subtracting the fluorescence image at 30 min from the image at 10 min followed by normalization to the total fluorescence. Conversely, disassembly of FAs was calculated by subtracting the fluorescence image at 10 min from the image at 30 min followed by normalization to the total fluorescence.

Fluorescence recovery after photobleaching (FRAP) measurements were performed on an Olympus Fluoview confocal laser-scanning microscope with a 100x water immersion objective. Single focal adhesions were photobleached for 2 sec at 100% of the 488 nm and 545 nm laser lines. Fluorescence recovery was recorded every 3 sec for two minutes and corrected to the fluorescence of an unbleached region. Fluorescence intensity at each time point was then normalized to the prebleached intensity of the FA.

2.6 Western blot analysis

Cells were lysed in urea buffer (4 M urea, 62.5 mM TrisCl, 2% SDS, 1 mM EDTA) containing a protease and phosphatase inhibitor cocktail (Sigma). Cell lysates were resolved with 12% SDS-PAGE. Proteins were transferred onto a nitrocellulose membrane, which was then subjected to two sequential incubations with appropriate primary antibodies (1:500 dilution for EBP50, pAKT, AKT and 1:1000 dilution for Flag, phospho-FAK, FAK, and EGF receptor (from Cell Signaling); 1:5000 dilution for β-actin (from Sigma)) followed by horseradish peroxidase-conjugated anti-mouse or anti-rabbit IgG antibody (1:2000 dilution, Cell signaling). Immunoreactivity was detected by incubation with Immune-Star ECL (Bio-Rad) on a Bio-Rad Molecular Imager. Quantitation of band intensity was performed with Image lab 4.0 (Bio-Rad) and Image J (National Institutes of Health).

For co-immunoprecipitation assay, cells were lysed in RIPA buffer (Santa Cruz) containing protease inhibitor cocktail. Lysates were incubated with the indicated antibodies for 2 h and with protein A/G beads overnight. Immuno-bead complexes were washed twice with NP-40 buffer (1 M Tris-base, 150 mM NaCl, 5 mM EDTA and 0.5% NP-40). Bound proteins were then released with 2× Laemmli sample buffer with 5% β-mercaptoethanol.

2.7 Statistical Analysis

Results from each experiment were averaged and expressed as mean ± standard error. Results were analyzed by ANOVA with Tukey's test or Student's t-test. Statistical calculations were performed with the GraphPad InStat3 software (GraphPad Software Inc., San Diego CA). P-values were considered statistically significant when lower than 0.05.

3. Results

3.1 EBP50 promotes VSMC spreading and migration

To begin characterizing the role of EBP50 on VSMC motility, we assessed the ability of WT and EBP50 KO primary VSMC to spread and migrate. Two hours after plating, VSMC from EBP50 KO mice displayed a more rounded and less spread phenotype than WT cells (Fig.

1A). However, after 24 h, both WT and KO cells were fully spread with well organized actin fibers (Fig 1A and B). Wound healing assays using primary VSMC isolated from WT and EBP50 KO mice cultured in the presence of 10% FBS demonstrated the significantly slower migration of KO cells (Fig 1C). A similar inhibition of migration was observed in VSMC in which EBP50 expression was inhibited by siRNA (Supplemental Figure 1). WT and KO VSMC have different proliferation rates [33]. Therefore, to establish if EBP50 directly regulates cell motility in these assays, the velocity of single cells during wound healing was determined by real-time recording of cell migration. As shown in Figure 1D, the velocity of KO cells was significantly lower than WT cells (10.4±0.9 vs. 20.5±1.2 μm/h, $p<10^{-7}$, for KO and WT cells, respectively). Collectively, these experiments indicate that EBP50 promotes VSMC spreading and migration.

3.2 EBP50 regulates focal adhesions (FAs)

Cell spreading and migration are dependent on the dynamic assembly and disassembly of focal adhesions. Focal adhesion kinase (FAK) is a key component of FAs and regulates the activity of a number of FA-associated proteins. To evaluate the effect of EBP50 on the distribution and number of FAs, WT and KO cells infected with an adenovirus GFP-tagged FAK (GFP-FAK) were analyzed by total internal reflection fluorescence (TIRF) microscopy. In WT cells FAK localized in focal contacts both at the periphery and throughout the surface of the cell (Fig. 2A). EBP50 KO cells showed changes in the distribution of focal adhesions, with adhesions being primarily at the cell's periphery (Fig. 2A). The number of FAs per unit area was significantly reduced in KO (Fig. 2B) and the size of FAs was significantly larger in KO cells (Fig. 2C). Endogenous FAK localization by confocal microscopy was performed in primary WT VSMC and following knock-down of EBP50 by a shRNA-expressing lentivirus. Similar to the previous observations, inhibition of EBP50 expression resulted in the reduction of the number of FA and their localization at the cell periphery (Fig. 2D). Co-staining for F-actin using phalloidin revealed the presence of well defined protrusions in control cells that are absent from shEBP50-treated cells (Fig. 2D).

The differences in size and distribution of FA in WT and KO cells suggest a selective reduction in nascent focal complexes in the latter cells. To confirm this, WT and KO cells were co-stained with vinculin (a marker of mature FA) and phospho-paxillin (a marker of nascent and mature adhesions). As shown in figure 2E, the percentage of phospho-paxillin that co-localizes with vinculin (i.e. Mander's coefficient) was significantly higher in KO cells.

The cellular distribution of EBP50 was characterized in VSMC expressing YFP-EBP50. EBP50 appeared distributed along fibers throughout the cell (Supplemental Figure 2). In addition, YFP fluorescence was present at the cell membrane, where FAK also localized (Supplemental Figure 2). However, there was no evidence of EBP50 in FAK-positive FAs.

3.3 EBP50 promotes EGF-induced migration and FA turnover in VSMC

Growth factors, such as EGF and platelet-derived growth factor (PDGF) are major stimuli for VSMC migration. To determine if EBP50 is specifically involved in growth factors-induced VSMC migration, wound-healing assays were performed with WT and KO cells in the absence or presence of EGF. The migration rate of KO cells was significantly slower than WT cells both in unstimulated cells and in EGF-treated cells (Fig. 3A). Similar effects were observed using Boyden chamber assays. As shown in Figure 3B, both EGF and PDGF stimulated migration of WT VSMC across the filter. In contrast, basal and growth factor-stimulated migration of KO VSMC was significantly reduced. Moreover, real time recording of isolated cells in the absence or presence of EGF revealed that the average velocity of WT

VSMC was significantly higher than that of KO cells (Fig. 3C and Supplemental Figure 3). Similar experiments performed in WT VSMC transfected with YFP-tagged EBP50 (YFP-EBP50) demonstrated that overexpression of EBP50 is sufficient to increased motility in response to EGF and PDGF (Fig. 3D).

During cell migration, focal adhesions are formed toward the leading edge of cells, while disassembly of adhesions occurs in the trailing edge of cells. To directly determine focal adhesion dynamics, cells expressing GFP-FAK were monitored in real-time by TIRF microscopy. The total number of FAs was rapidly reduced by EGF treatment in WT VSMC, whereas no significant change in the number of FAs was observed in KO cells (Fig. 4A). To visualize FA remodeling in response to EGF, images taken at t=10 (in red) and t=30 min (in green) were superimposed (Fig. 4B). Both newly assembled FAs (in green) and disassembled FAs (in red) were increased in WT cells, whereas the number of stable FAs (in yellow) in KO cells was greater than in WT cells. Representative time-lapse images of FA remodeling at the leading and trailing edges of a WT cell are shown in figure 4C. Quantitative analysis of these experiments indicates that both FA assembly and disassembly were reduced in KO cells compared to WT cells (Fig. 4D).

3.4 EBP50 potentiates the interaction between EGFR and FAK

The previous experiments indicate that EBP50 regulates VSMC motility by potentiating growth factor-induced FA dynamic. Indeed, EBP50 functions as a scaffold between PDGF receptor and FAK [35]. Moreover, EBP50 associates with EGFR [12, 36]. We therefore determined if EBP50 forms a complex with EGFR and FAK in VSMC. To this end, immunoprecipitation assays were performed in primary VSMC expressing Flag-tagged EBP50. As shown in Fig. 5A, both FAK and EGFR interacted with EBP50. To determine the specific domain in EBP50 that mediate the interaction with EGFR, co-immunoprecipitation experiments were performed in CHO cells (that do not express endogenous EBP50) transfected with EBP50 variants harboring inactivating mutations in PDZ1 (S1) or PDZ2 (S2) (Fig. 5B). As shown in figure 5C, EGFR interacted equivalently with WT and S1 mutant EBP50, whereas the interaction was abolished with the S2 mutant. Thus, in intact cells EGFR interacts with the PDZ2 of EBP50. Similar experiments were performed with FAK. In addition to the S1 and S2 mutants, EBP50 variants containing mutations in both PDZ domains (S1/S2) and a truncated form of EBP50 lacking the C-terminal ERM domain (ΔERM) were used. FAK co-immunoprecipitated with WT EBP50 and with S1, S2 and S1/S2 mutants, but failed to interact with the ΔERM (Fig. 5D). This experiment demonstrates that the interaction between FAK and EBP50 is mediated by the ERM domain.

The preceding studies suggest the possibility that EBP50, EGFR and FAK are part of a signaling complex. The presence of a ternary complex was tested by immunoprecipitating HA-FAK and monitoring the presence of EGFR in WT and KO VSMC. As shown in figure 6A, the formation of the complex between EGFR and FAK (determined by co-immunoprecipitation of HA-FAK followed by immunoblotting for EGFR) was significantly reduced in KO cells (25.1±3.2 % vs. WT, p=0.002, N=3), indicating that EBP50 functions as a scaffold between EGFR and FAK. Reverse experiments were performed in CHO cells (that do not express EBP50). In naïve CHO cells, FAK did not co-immunoprecipitate with EGFR (Fig. 6B). However, consistent with the findings in VSMC, expression of EBP50 increased the interaction between EGFR and FAK. Furthermore, and in agreement with the previous analysis, while both WT EBP50 and S1 mutant were able to scaffold EGFR and FAK, the formation of the ternary complex was lost with S2 and ΔERM mutants (Fig. 6C). Collectively, these studies show that EBP50 promotes the recruitment of FAK into an EGFR-containing complex.

3.5 EBP50 increases EGF-dependent FAK phosphorylation

The activity of FAK is primarily regulated by phosphorylation on tyrosine residues. In particular, integrin-dependent auto-phosphorylation of Tyr-397 results in the recruitment of src and the additional phosphorylation of Tyr-925. The latter event is important for growth factors-induced cell motility. To determine if EBP50 contributes to FAK phosphorylation, WT and KO cells grown in 10% FBS culture media were lysed and blotted for phospho-specific FAK antibodies. As shown in figure 7A, no differences in total FAK expression and in Tyr-397 phosphorylation were observed in WT and KO cells. In contrast, phosphorylation of Tyr-925 was significantly greater in WT than in KO cells (Fig. 7B). Similar results were obtained in WT VSMC in which EBP50 expression was inhibited by lentiviral delivery of shRNA (Supplemental Figure 4A). In addition, Tyr-925 phosphorylation was increased in cells overexpressing YFP-EBP50 (Fig. 7C). Treatment of WT VSMC with EGF resulted in a time- and dose-dependent increase in FAK-Y925 phosphorylation, which was significantly reduced in KO cells (Fig. 7D) and in cells treated with siEBP50 (Supplemental Figure 4B). However, stimulation with fibroblast growth factor (FGF) elicited similar FAK-Y925 phosphorylation in WT and KO cells (Supplemental Figure 4C), indicating that KO cells are fully competent for phosphorylation of FAK.

Phosphorylation of Tyr-925 increases the residence time of FAK in FA, thus increasing its ability to regulate FA turnover [19]. To study the effect of EBP50 on FAK dynamics, fluorescence recovery after photobleaching (FRAP) experiments were performed in WT and KO cells expressing GFP-FAK. Single FAs at the cell periphery were photobleached and the recovery of fluorescence was followed in real time (Fig. 8). The recovery of FAK fluorescence was significantly slower in WT cells compared to KO cells ($t_{1/2}$ = 30.2±5.9 s vs. 15.3±2.7 s, $p<0.03$, for WT and KO, respectively). These results indicate that EBP50, by promoting Tyr-925 phosphorylation, increases the residence time of FAK in FA, thus promoting FA turnover.

4. Discussion

The studies presented here were prompted by the observation that EBP50 expression increases in VSMC following endothelial injury and exacerbates neointimal hyperplasia [32, 33]. Smooth muscle cell migration occurs in response to vascular injury and during atherogenesis [5, 6]. This process is driven by growth factors and cytokines that are released locally during vascular remodeling. In atherogenesis, VSMC migrate from the media to the lesion where they contribute to arterial thickening, extracellular matrix deposition and affect the stability of the atheroma. Similarly, the increased neointima formation that often follows angioplasty has been attributed to increased VSMC proliferation and migration from the media to the intima. We hypothesized that the reduction in neointima formation observed in EBP50 knockout mice derives, in addition to reduced VSMC proliferation [33], from a direct effect of EBP50 on VSMC motility.

The role of EBP50 on cell migration has been examined in a various cell types. In neuroblastoma cells, EBP50 depletion inhibited migration [29]. In contrast, EBP50 decreased motility of colorectal cancer cells [37]. The migration in response to PDGF was increased in EBP50-null embryonic fibroblasts compared to wild type cells [38]. In this system, EBP50 inhibited PI3K activity by scaffolding the PDGF receptor and PTEN. However, a mutation in the PDGF receptor that prevents its interaction with EBP50 resulted in reduced migration and spreading of mouse embryonic fibroblasts [35]. In this case, EBP50 increased phosphorylation of FAK and potentiated both PDGF- and integrin-induced motility. In rat VSMC, siRNA-mediated depletion of EBP50 increased migration in unstimulated (i.e serum-free) conditions, an effect attributed to the scaffolding of myosin IIa and the microtubule network [39]. Therefore, the effect of EBP50 on cell motility is

remarkably cell-specific and considerable controversy remains regarding the molecular mediators underlying these actions.

The experiments described here show that EBP50 promotes the formation of a complex containing EGFR and FAK. The formation of this signaling complex facilitates the phosphorylation of FAK on Tyr-925 in response to EGF. Consistent with previous reports [19] phosphorylation at this site increases the residence time of FAK in FAs resulting in higher FA turnover and promoting cell motility. The scaffolding role of EBP50 for EGFR and FAK is consistent with previous reports showing that the interaction between growth factor receptors and FAK requires an accessory protein [12] and that EBP50 is necessary for the association of PDGFR and FAK [35]. Our analyses indicated that the interaction with FAK is mediated by the C-terminal ERM domain of EBP50, whereas the interaction with EGFR occurs at the PDZ2 domain. The use of two distinct domains therefore allows EBP50 to scaffold EGFR and FAK in a common complex. Previous work by Lazar et al. indicated that the interaction between EGFR and EBP50 involves the PDZ1 domain of EBP50 [36]. It is possible that the preference of EGFR for a specific PDZ domain depends on the cellular context. In particular, it is now clear that phosphorylation of EBP50 by a number of kinases (including GRK6a, PKC and PKA) profoundly affects its interactions [40–43]. Also, the C-terminal sequence of EBP50 is a PDZ ligand itself and evidence supports the interaction between this PDZ-binding motif and the PDZ2 domain, resulting in a “closed” conformation [44–46]. It is therefore possible that the engagement of the C-terminal ERM domain by other proteins (such as FAK) may unmask a high affinity state for the PDZ2 domain [47–49]. It is also relevant to observe that EBP50 promotes the formation of leading-edge pseudopodia in breast cancer cells through effects mediated by its PDZ2 domain [50].

We demonstrate that EBP50, by promoting the interaction between FAK and EGFR, directly affects FAK activation. Although the phosphorylation of FAK at Tyr-397 was similar in WT and KO cells, a significant reduction of phosphorylation at Tyr-925, which is primarily mediated by members of the src family, occurred in EBP50 null cells. The importance of Tyr-925 phosphorylation for cell migration has been demonstrated recently. Expression of the mutant Y925F-FAK did not rescue migration of FAK-null fibroblasts [19]. Moreover, Tyr-925 phosphorylation increases the residence time of FAK in FAs [19], which is consistent with our observations in primary VSMC. Therefore, both the phenotypic changes associated with the loss of EBP50 in VSMC and the effect of EBP50 on FAK dynamics are remarkably similar to those described for the Y925F-FAK mutant.

FAs consist of a complex of proteins that form dynamic structures within the cell. The coordinated assembly and disassembly of FAs is required for cell motility. Here we show that EBP50 plays a key role in the regulation of FAs. EBP50 null cells have defects in the organization, number and size of FAs, and in their dynamic assembly and disassembly. EBP50 null cells have larger FAs distributed at the cell periphery. This type of adhesions has been described in FAK-null keratinocytes [11], and is characteristic of stable FAs in non-migrating cells. In contrast, smaller dynamic FAs were observed in WT VSMC. The decreased FA assembly and disassembly in KO cells upon EGF stimulation underlines the importance of EBP50 in regulating growth factors-induced FA remodeling. Interestingly, this effect is likely not exclusive for EGFR. Indeed, EBP50 interacts with the PDGFR in embryonic fibroblasts and, consistent with our observations in VSMC, regulates spreading and migration in response to PDGF [35].

The actions of EBP50 on FAK activation and FA dynamics have important consequences on VSMC motility. In contrast to a recent report in rat VSMC [39], our studies indicate that EBP50 promotes migration of murine VSMC. The major difference in the experimental designs that may account for these opposite effects is the absence or presence of growth

factors. Indeed, in the study from Baeyens, cells were maintained in the absence of serum for 24–48 h, whereas in our experiments cells were either stimulated with growth factors (EGF, PDGF or serum) or remained in 0.1% FBS for a maximum of 16 h. Importantly, EBP50 is phosphorylated at several sites by a variety of kinases (including PKA, PKC and GRK6) and EBP50 phosphorylation profoundly affects its function (recently reviewed in [51]). It is therefore possible that different experimental conditions, in particular prolonged absence of stimuli, result in distinct phosphorylation patterns, and consequently functions, of EBP50.

The effect of EBP50 on VSMC migration was confirmed in different experimental modalities, including the use of EBP50 KO cells, the inhibition of EBP50 expression by both siRNA and lentiviral shRNA, and conversely by overexpression of EBP50. These complementary approaches strongly indicate that the inhibition of migration in the absence of EBP50 is specific and not due to off-target effects of the experimental manipulations. Moreover, real-time imaging of migrating VSMC allowed for the measurement of the velocity of single cells, which was significantly reduced in KO cells. These experiments are important because of the contribution of proliferation and cell density to the assessment of migration by “wound healing” assays.

In summary, the studies described here define the role of EBP50 in the regulation of growth factor-induced FAK activation, FA dynamics and VSMC motility. These studies are particularly relevant in light of the emerging role for EBP50 on vascular remodeling. EBP50 expression increases upon vascular injury and contributes to neointimal hyperplasia. Conversely, EBP50 null mice are protected from injury-induced neointima formation. The temporal expression of EBP50 in injured vessels and its actions on VSMC proliferation and migration indicate that this scaffolding protein plays a critical role in the response of vessels to injury.

Supplementary Material

Refer to Web version on PubMed Central for supplementary material.

Acknowledgments

We thank Dr. Timothy Feinstein (University of Pittsburgh) for assistance in the TIRF experiments; and Drs. Bin Wang, Peter Friedman, Alexander Sorkin (University of Pittsburgh), Dr. David Schaepfer (University of California San Diego) and Dr. Harold Singer (Albany Medical College) for providing reagents.

This work was supported in part the American Heart Association Great River Grant-in-Aid 10BGIA350005 (to GJS), a Pilot Project Program in Hemostasis and Vascular Biology - Vascular Medicine Institute, University of Pittsburgh - supported by grants from the Institute for Transfusion Medicine and the Hemophilia Society of Western Pennsylvania (to AB), the National Institutes of Health through Grant Numbers UL1 RR024153 and UL1TR000005. Kristen Leslie is supported by the NIH pre-doctoral training grant T32GM08424.

Abbreviations

EBP50	Ezrin-Radixin-Moesin-Binding Phosphoprotein 50
EGF	epidermal growth factor
EGFR	EGF receptor
ERM	Ezrin-Radixin-Moesin
FA	focal adhesion
FAK	focal adhesion kinase

FBS	fetal bovine serum
GFP	green fluorescent protein
KO	knockout
PDZ	postsynaptic density 95/discs large/zona occludens
VSMC	vascular smooth muscle cell
WT	wild type
YFP	yellow fluorescent protein

References

1. Aman A, Piotrowski T. Cell migration during morphogenesis. Dev Biol. 2010; 341:20–33. [PubMed: 19914236]
2. Friedl P, Gilmour D. Collective cell migration in morphogenesis, regeneration and cancer. Nat Rev Mol Cell Biol. 2009; 10:445–457. [PubMed: 19546857]
3. Sanz-Moreno V, Marshall CJ. The plasticity of cytoskeletal dynamics underlying neoplastic cell migration. Curr Opin Cell Biol. 2010; 22:690–696. [PubMed: 20829016]
4. Makrilia N, Kollias A, Manolopoulos L, Syrigos K. Cell adhesion molecules: role and clinical significance in cancer. Cancer Invest. 2009; 27:1023–1037. [PubMed: 19909018]
5. Louis SF, Zahradka P. Vascular smooth muscle cell motility: From migration to invasion. Exp Clin Cardiol. 2010; 15:e75–e85. [PubMed: 21264073]
6. Gerthoffer WT. Mechanisms of vascular smooth muscle cell migration. Circ Res. 2007; 100:607–621. [PubMed: 17363707]
7. Romer LH, Birukov KG, Garcia JG. Focal adhesions: paradigm for a signaling nexus. Circ Res. 2006; 98:606–616. [PubMed: 16543511]
8. Webb DJ, Donais K, Whitmore LA, Thomas SM, Turner CE, Parsons JT, et al. FAK-Src signalling through paxillin, ERK and MLCK regulates adhesion disassembly. Nat Cell Biol. 2004; 6:154–161. [PubMed: 14743221]
9. Iwanicki MP, Vomastek T, Tilghman RW, Martin KH, Banerjee J, Wedegaertner PB, et al. FAK, PDZ-RhoGEF and ROCKII cooperate to regulate adhesion movement and trailing-edge retraction in fibroblasts. J Cell Sci. 2008; 121:895–905. [PubMed: 18303050]
10. Zaidel-Bar R, Itzkovitz S, Ma'ayan A, Iyengar R, Geiger B. Functional atlas of the integrin adhesome. Nat Cell Biol. 2007; 9:858–867. [PubMed: 17671451]
11. Schober M, Raghavan S, Nikolova M, Polak L, Pasolli HA, Beggs HE, et al. Focal adhesion kinase modulates tension signaling to control actin and focal adhesion dynamics. J Cell Biol. 2007; 176:667–680. [PubMed: 17325207]
12. Sieg DJ, Hauck CR, Ilic D, Klingbeil CK, Schaefer E, Damsky CH, et al. FAK integrates growth-factor and integrin signals to promote cell migration. Nat Cell Biol. 2000; 2:249–256. [PubMed: 10806474]
13. Gilmore AP, Romer LH. Inhibition of focal adhesion kinase (FAK) signaling in focal adhesions decreases cell motility and proliferation. Mol Biol Cell. 1996; 7:1209–1224. [PubMed: 8856665]
14. Sieg DJ, Hauck CR, Schlaepfer DD. Required role of focal adhesion kinase (FAK) for integrin-stimulated cell migration. J Cell Sci. 1999; 112:2677–2691. [PubMed: 10413676]
15. Ilic D, Furuta Y, Kanazawa S, Takeda N, Sobue K, Nakatsuji N, et al. Reduced cell motility and enhanced focal adhesion contact formation in cells from FAK-deficient mice. Nature. 1995; 377:539–544. [PubMed: 7566154]
16. Schaller MD, Hildebrand JD, Shannon JD, Fox JW, Vines RR, Parsons JT. Autophosphorylation of the focal adhesion kinase, pp125FAK, directs SH2-dependent binding of pp60src. Mol Cell Biol. 1994; 14:1680–1688. [PubMed: 7509446]

17. Calalb MB, Polte TR, Hanks SK. Tyrosine phosphorylation of focal adhesion kinase at sites in the catalytic domain regulates kinase activity: a role for Src family kinases. Mol Cell Biol. 1995; 15:954–963. [PubMed: 7529876]
18. Schlaepfer DD, Hunter T. Evidence for in vivo phosphorylation of the Grb2 SH2-domain binding site on focal adhesion kinase by Src-family protein-tyrosine kinases. Mol Cell Biol. 1996; 16:5623–5633. [PubMed: 8816475]
19. Deramaudt TB, Dujardin D, Hamadi A, Noulet F, Kolli K, De Mey J, et al. FAK phosphorylation at Tyr-925 regulates cross-talk between focal adhesion turnover and cell protrusion. Mol Biol Cell. 2011; 22:964–975. [PubMed: 21289086]
20. Romero G, von Zastrow M, Friedman PA. Role of PDZ proteins in regulating trafficking, signaling, and function of GPCRs: means, motif, and opportunity. Adv Pharmacol. 2011; 62:279–314. [PubMed: 21907913]
21. Weinman EJ, Steplock D, Wang Y, Shenolikar S. Characterization of a protein cofactor that mediates protein kinase A regulation of the renal brush border membrane Na(+)-H(+) exchanger. J Clin Invest. 1995; 95:2143–2149. [PubMed: 7738182]
22. Seidler U, Singh AK, Cinar A, Chen M, Hillesheim J, Hogema B, et al. The role of the NHERF family of PDZ scaffolding proteins in the regulation of salt and water transport. Ann N Y Acad Sci. 2009; 1165:249–260. [PubMed: 19538313]
23. Blaine J, Weinman EJ, Cunningham R. The regulation of renal phosphate transport. Adv Chronic Kidney Dis. 2011; 18:77–84. [PubMed: 21406291]
24. Kato A, Romero MF. Regulation of electroneutral NaCl absorption by the small intestine. Annu Rev Physiol. 2011; 73:261–281. [PubMed: 21054167]
25. Fouassier L, Rosenberg P, Mergey M, Saubamea B, Claperon A, Kinnman N, et al. Ezrin-radixin-moesin-binding phosphoprotein (EBP50), an estrogen-inducible scaffold protein, contributes to biliary epithelial cell proliferation. Am J Pathol. 2009; 174:869–880. [PubMed: 19234136]
26. Li M, Wang W, Soroka CJ, Mennone A, Harry K, Weinman EJ, et al. NHERF-1 binds to Mrp2 and regulates hepatic Mrp2 expression and function. J Biol Chem. 2010; 285:19299–19307. [PubMed: 20404332]
27. Song J, Bai J, Yang W, Gabrielson EW, Chan DW, Zhang Z. Expression and clinicopathological significance of oestrogen-responsive ezrin-radixin-moesin-binding phosphoprotein 50 in breast cancer. Histopathology. 2007; 51:40–53. [PubMed: 17593079]
28. Shibata T, Chuma M, Kokubu A, Sakamoto M, Hirohashi S. EBP50, a beta-catenin-associating protein, enhances Wnt signaling and is over-expressed in hepatocellular carcinoma. Hepatology. 2003; 38:178–186. [PubMed: 12830000]
29. Kislin KL, McDonough WS, Eschbacher JM, Armstrong BA, Berens ME. NHERF-1: modulator of glioblastoma cell migration and invasion. Neoplasia. 2009; 11:377–387. [PubMed: 19308292]
30. Hayashi Y, Molina JR, Hamilton SR, Georgescu MM. NHERF1/EBP50 is a new marker in colorectal cancer. Neoplasia. 12:1013–1022. [PubMed: 21170265]
31. Baeyens N, Horman S, Vertommen D, Rider M, Morel N. Identification and functional implication of a Rho kinase-dependent moesin-EBP50 interaction in noradrenaline-stimulated artery. Am J Physiol Cell Physiol. 2010; 299:C1530–C1540. [PubMed: 20926777]
32. Song GJ, Barrick S, Leslie KL, Sicari B, Fiaschi-Taesch NM, Bisello A. EBP50 inhibits the anti-mitogenic action of the parathyroid hormone type 1 receptor in vascular smooth muscle cells. J Mol Cell Cardiol. 2010; 49:1012–1021. [PubMed: 20843475]
33. Song GJ, Barrick S, Leslie KL, Bauer PM, Alonso V, Friedman PA, et al. The scaffolding protein EBP50 promotes vascular smooth muscle cell proliferation and neointima formation by regulating Skp2 and p21(cip1). Arterioscler Thromb Vasc Biol. 2012; 32:33–41. [PubMed: 22034511]
34. Bolte S, Cordelieres FP. A guided tour into subcellular colocalization analysis in light microscopy. J Microsc. 2006; 224:213–232. [PubMed: 17210054]
35. James MF, Beauchamp RL, Manchanda N, Kazlauskas A, Ramesh V. A NHERF binding site links the betaPDGFR to the cytoskeleton and regulates cell spreading and migration. J Cell Sci. 2004; 117:2951–2961. [PubMed: 15161943]

36. Lazar CS, Cresson CM, Lauffenburger DA, Gill GN. The Na+/H+ exchanger regulatory factor stabilizes epidermal growth factor receptors at the cell surface. Mol Biol Cell. 2004; 15:5470–5480. [PubMed: 15469991]
37. Hayashi Y, Molina JR, Hamilton SR, Georgescu MM. NHERF1/EBP50 is a new marker in colorectal cancer. Neoplasia. 2010; 12:1013–1022. [PubMed: 21170265]
38. Takahashi Y, Morales FC, Kreimann EL, Georgescu MM. PTEN tumor suppressor associates with NHERF proteins to attenuate PDGF receptor signaling. EMBO J. 2006; 25:910–920. [PubMed: 16456542]
39. Baeyens N, de Meester C, Yerna X, Morel N. EBP50 is involved in the regulation of vascular smooth muscle cell migration and cytokinesis. J Cell Biochem. 2011; 112:2574–2584. [PubMed: 21598299]
40. Hall RA, Spurney RF, Premont RT, Rahman N, Blitzer JT, Pitcher JA, et al. G protein-coupled receptor kinase 6A phosphorylates the Na(+)/H(+) exchanger regulatory factor via a PDZ domain-mediated interaction. J Biol Chem. 1999; 274:24328–24334. [PubMed: 10446210]
41. Voltz JW, Brush M, Sikes S, Steplock D, Weinman EJ, Shenolikar S. Phosphorylation of PDZ1 domain attenuates NHERF-1 binding to cellular targets. J Biol Chem. 2007; 282:33879–33887. [PubMed: 17895247]
42. Weinman EJ, Steplock D, Zhang Y, Biswas R, Bloch RJ, Shenolikar S. Cooperativity between the phosphorylation of Thr95 and Ser77 of NHERF-1 in the hormonal regulation of renal phosphate transport. J Biol Chem. 2010; 285:25134–25138. [PubMed: 20571032]
43. Fouassier L, Nichols MT, Gidey E, McWilliams RR, Robin H, Finnigan C, et al. Protein kinase C regulates the phosphorylation and oligomerization of ERM binding phosphoprotein 50. Exp Cell Res. 2005; 306:264–273. [PubMed: 15878350]
44. Li J, Poulikakos PI, Dai Z, Testa JR, Callaway DJ, Bu Z. Protein kinase C phosphorylation disrupts Na+/H+ exchanger regulatory factor 1 autoinhibition and promotes cystic fibrosis transmembrane conductance regulator macromolecular assembly. J Biol Chem. 2007; 282:27086–27099. [PubMed: 17613530]
45. Raghuram V, Hormuth H, Foskett JK. A kinase-regulated mechanism controls CFTR channel gating by disrupting bivalent PDZ domain interactions. Proc Natl Acad Sci USA. 2003; 100:9620–9625. [PubMed: 12881487]
46. Morales FC, Takahashi Y, Momin S, Adams H, Chen X, Georgescu MM. NHERF1/EBP50 head-to-tail intramolecular interaction masks association with PDZ domain ligands. Mol Cell Biol. 2007; 27:2527–2537. [PubMed: 17242191]
47. Reczek D, Bretscher A. The carboxyl-terminal region of EBP50 binds to a site in the amino-terminal domain of ezrin that is masked in the dormant molecule. J Biol Chem. 1998; 273:18452–18458. [PubMed: 9660814]
48. Li J, Callaway DJ, Bu Z. Ezrin induces long-range interdomain allostery in the scaffolding protein NHERF1. J Mol Biol. 2009; 392:166–180. [PubMed: 19591839]
49. Li J, Dai Z, Jana D, Callaway DJ, Bu Z. Ezrin controls the macromolecular complexes formed between an adapter protein Na+/H+ exchanger regulatory factor and the cystic fibrosis transmembrane conductance regulator. J Biol Chem. 2005; 280:37634–37643. [PubMed: 16129695]
50. Cardone RA, Bellizzi A, Busco G, Weinman EJ, Dell'Aquila ME, Casavola V, et al. The NHERF1 PDZ2 domain regulates PKA-RhoA-p38-mediated NHE1 activation and invasion in breast tumor cells. Mol Biol Cell. 2007; 18:1768–1780. [PubMed: 17332506]
51. Ardura JA, Friedman PA. Regulation of G protein-coupled receptor function by Na+/H+ exchange regulatory factors. Pharmacol Rev. 2011; 63:882–900. [PubMed: 21873413]

Highlights

- The PDZ-containing scaffolding protein EBP50 promotes vascular smooth muscle cell migration
- EBP50 scaffolds the interaction between EGFR and FAK resulting in increased FAK phosphorylation
- EBP50 regulates focal adhesion dynamics
- These effects expand the understanding of the role of EBP50 on vascular remodeling

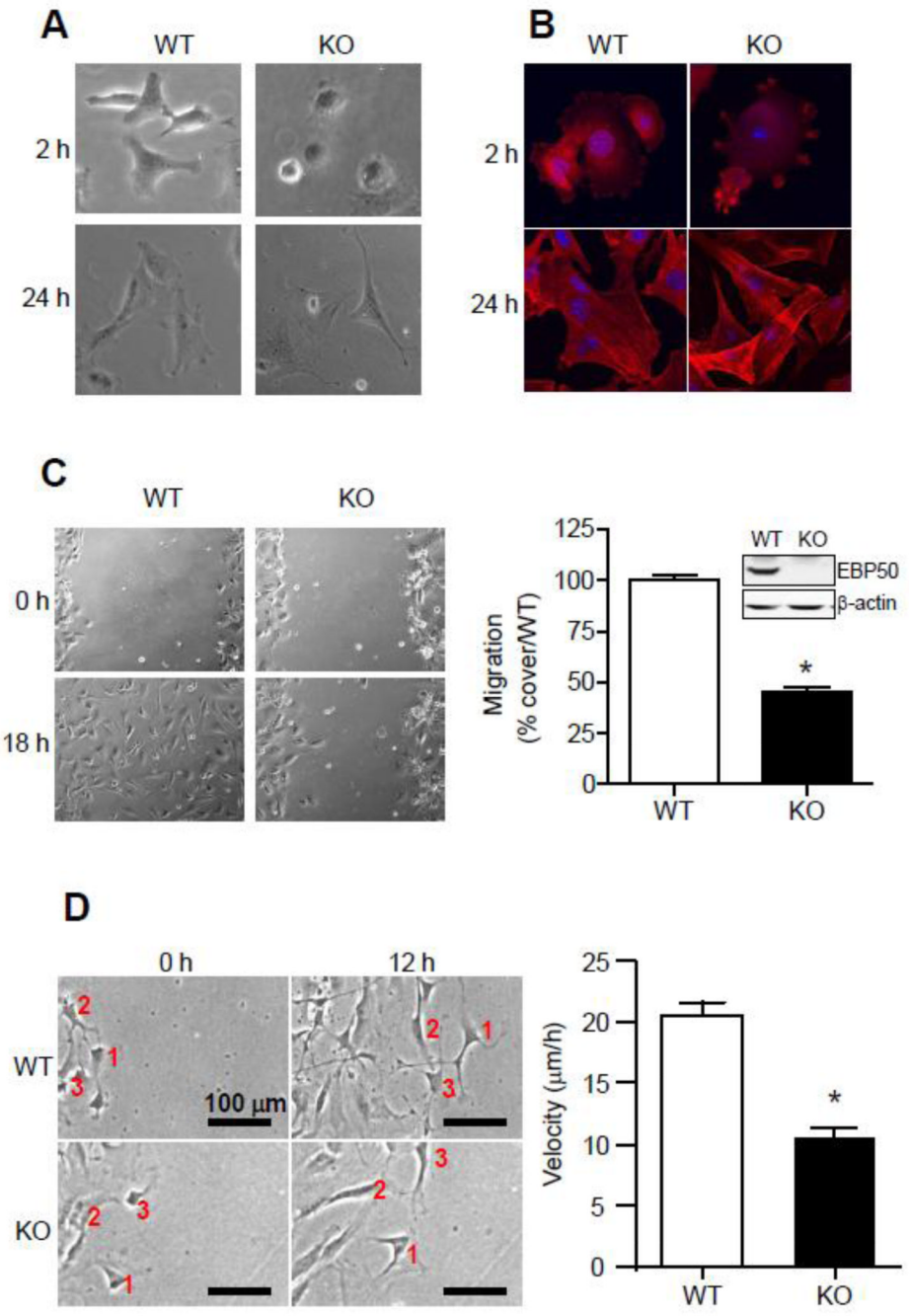

Figure 1. EBP50 promotes spreading and migration of vascular smooth muscle cells

A. Delayed spreading of EBP50 KO VSMC. Equal number of primary VSMC from WT and EBP50 KO mice were seeded on plastic dishes and bright field micrographs acquired after 2 and 24 h. **B**. Primary VSMC from WT and EBP50 KO mice were fixed 2 and 24 h after seeding and stained with phalloidin. **C**. Confluent cultures of WT and KO VSMC were scratched with a sterile tip to generate a wound area. Cells were maintained in DMEM supplemented with 10% FBS and micrographs were obtained at the indicated times. Graph shows percent covered area relative to WT after 20 h. *, $p<0.05$, N=4. Insert shows the expression of EBP50 in WT and KO cells. **D**. Migration of WT and KO cells was recorded

in real time over 20 h. Panels shows representative images of three cells (numbered) at time zero and after 12 h. Graph shows the average velocity of single WT and KO cells. *, $p<10^{-7}$, N=20.

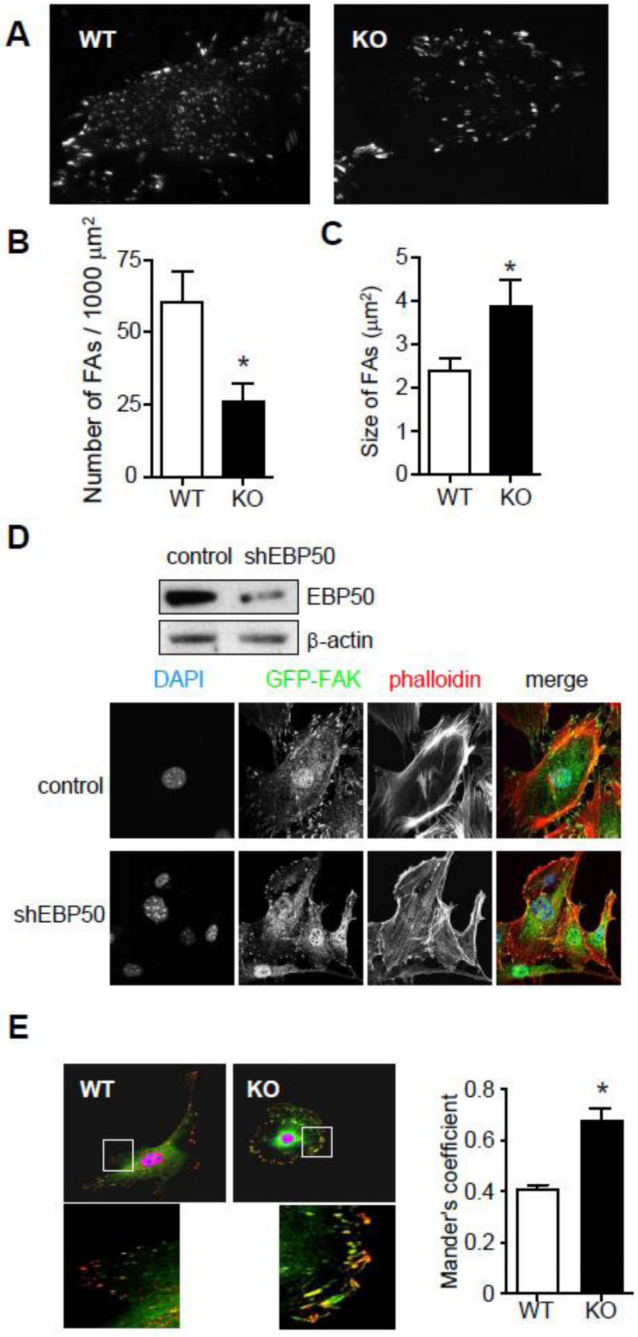

Figure 2. EBP50 regulates focal adhesions

A. VSMC WT and KO cells infected with adenovirus for GFP-FAK were plated on cover slips. Localization of GFP-FAK in focal adhesions and its mobilization was monitored by TIRF microscopy. The number (**B**) and the size (**C**) of focal adhesions in WT and KO cells were measured. *, P <0.05, N=7. **D**. VSMC cells infected with lentivirus expressing shRNA for EBP50 and control vector (top panel) were fixed and stained for endogenous FAK (green) and F-actin (phalloidin, in red). **E.** VSMC WT and KO cells were fixed and stained for vinculin (green) and phospho-paxillin (red). Graph shows the fraction of phospho-paxillin that co-localizes with vinculin (Mander's coefficient). *, P<0.008, N=6.

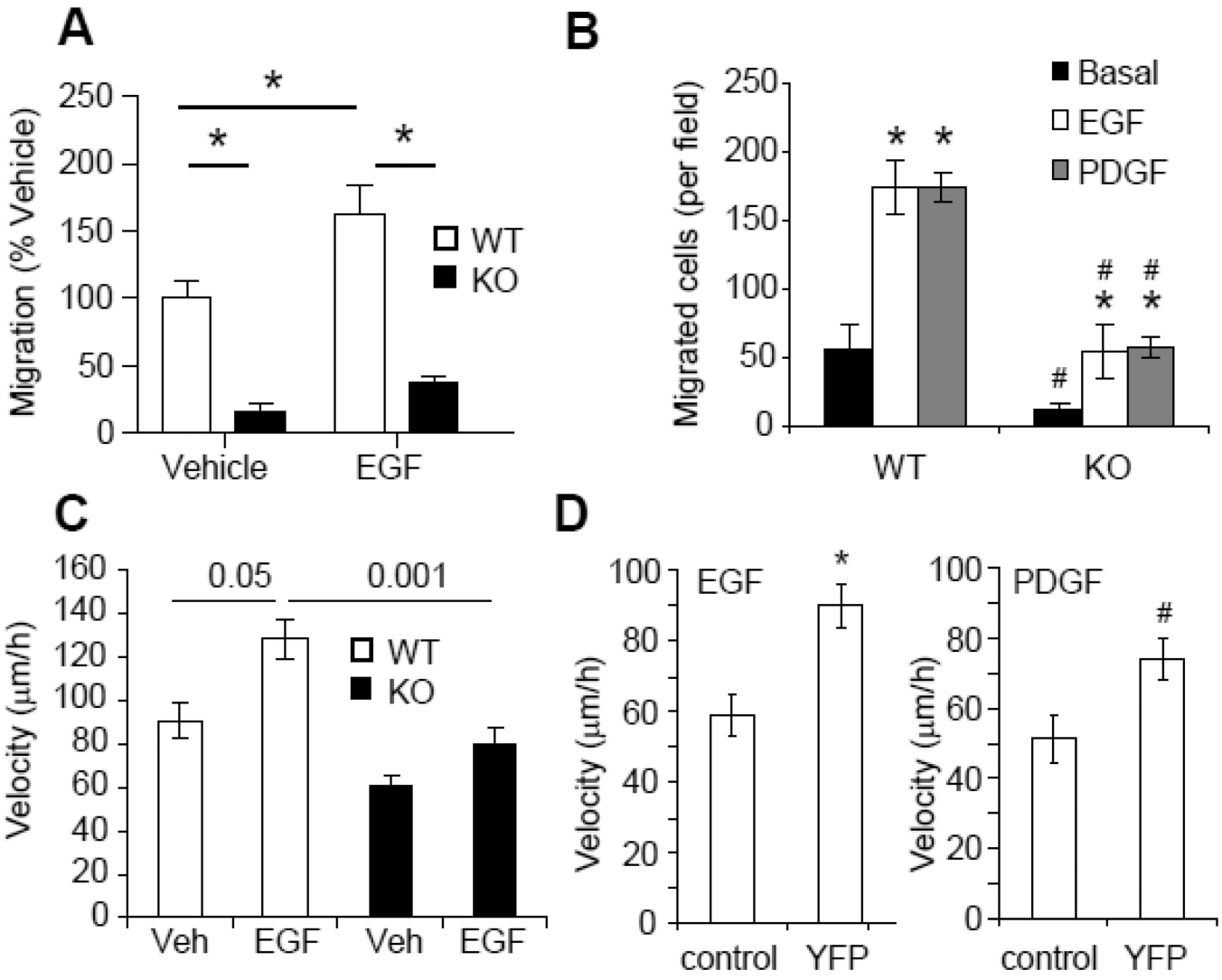

Figure 3. EBP50 regulates growth-factors-induced cell motility FA dynamic

A. Monolayers of WT and KO cells were scratched and incubated in 0.1% FBS without (Vehicle) or with 10 ng/ml EGF. Cell migration was monitored over 20 h. Graph shows the mean values ± SE of recovered wound area relative to WT vehicle-treated cells. *, $p < 0.05$, N=4. **B.** Equal numbers (5×10^4 cells) of WT and KO VSMC were plated on the upper compartment of a Boyden chamber and cell migration towards EGF (10 ng/ml) or (PDGF 10 ng/ml) was quantitated after 5 h at 37 °C. Graph shows the number of migrated cells. *, $P<0.01$ vs. basal; #, $P<0.0004$ vs. WT, N=4. **C.** Migration of isolated WT and KO cells was recorded in real time over 12 h in the absence or presence of EGF (10 ng/ml). Graph shows the average velocity of single WT and KO cells. P values are indicated, N=11. **D.** Migration of isolated WT VSMC electroporated with pcDNA3(control) or EBP50-YFP was recorded in real time over 12 h. Graph shows the average velocity of single cells in the presence of EGF (10 ng/ml) or PDGF (10 ng/ml). *, $p<0.0007$, #, $p<0.004$ vs. vehicle, N=7.

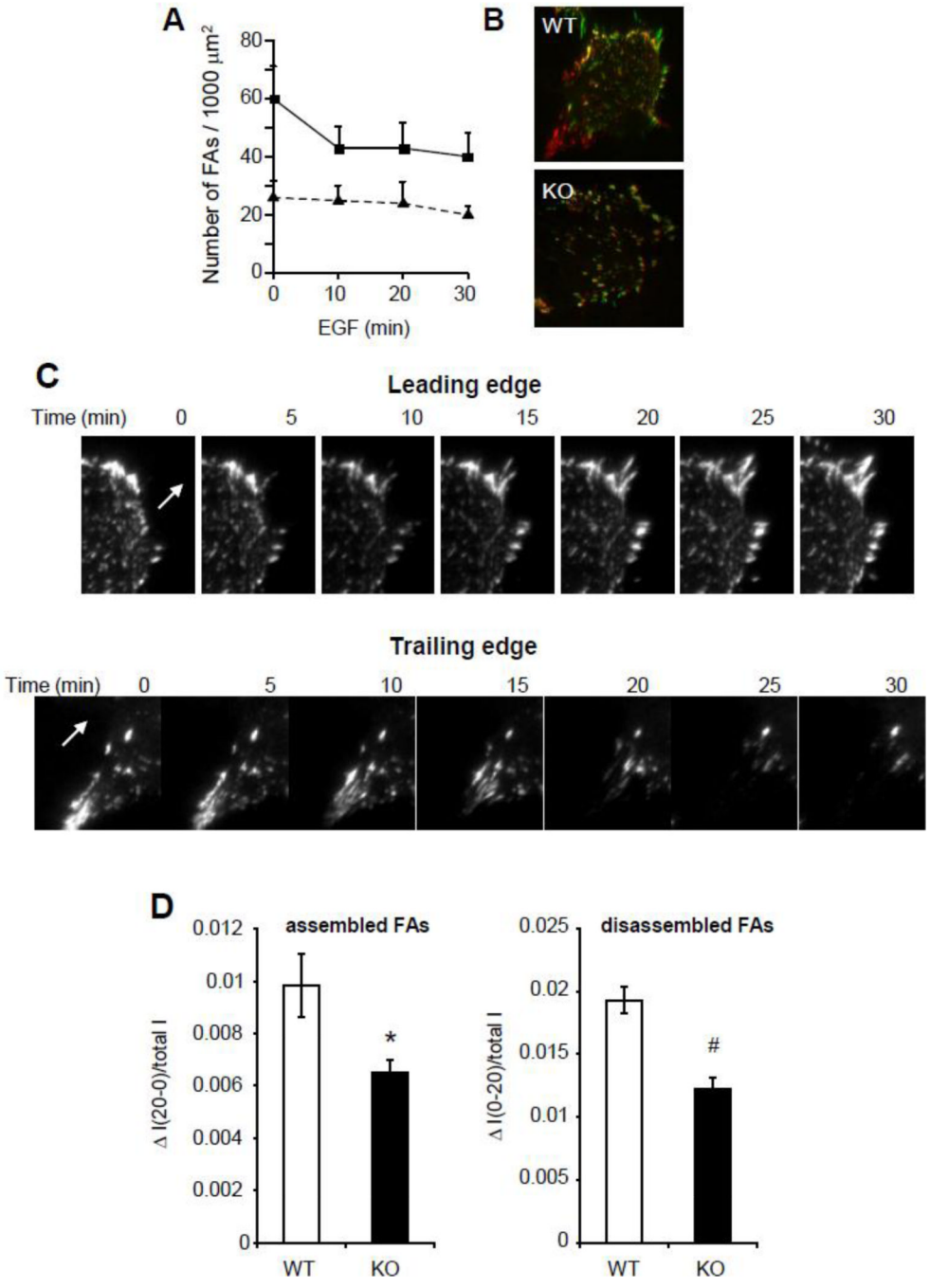

Figure 4. EBP50 regulates FA dynamic

A. WT and KO VSMC infected with GFP-FAK adenovirus were plated on cover slips and incubated in 0.1% FBS overnight. GFP-FAK localization was monitored in real time by TIRF microscopy following treatment with 10 ng/ml EGF. Graph shows the average number ± SE of FAs per unit of cell area following EGF treatment. **B.** EGF-treated WT and KO cells expressing GFP-FAK were monitored by TIRF microscopy. Pictures of WT and KO cells were pseudo-colored in red (10 min after EGF) and in green (30 min after EGF) and merged. Green and red fluorescence represent newly assembled and disassembled FAs, respectively. Yellow fluorescence represents stable FAs. **C**. Representative images of the leading edge

(upper panels) and trailing edge (lower panels) of VSMC expressing GFP-FAK and monitored every 5 min for 60 min by TIRF microscopy. The arrows indicate the direction of motion. **D**. Assembly and disassembly of FAs over 20 min was calculated in cells from D as described in the Methods. *, $p<0.02$ and #, $p<0.002$, N=10.

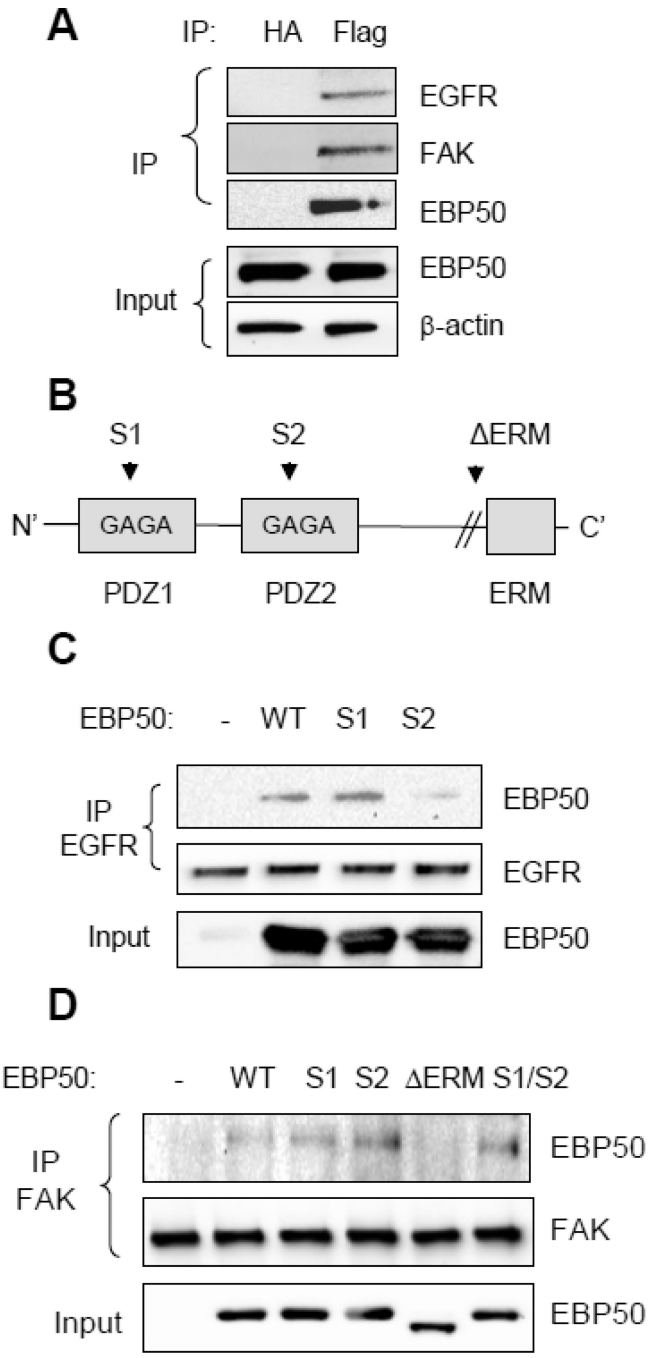

Figure 5. EBP50 interactions with EGFR and FAK

A. VSMC expressing Flag-EBP50 were lysed and immunoprecipitation experiments performed with control anti-HA or anti-Flag antibodies. The immunoprecipitate (IP) or lysates prior to immunoprecipitation (input) were analyzed by Western blot with anti-EGFR, anti-FAK or anti-EBP50 antibodies. EBP50 coimmunoprecipitates with both FAK and EGFR. **B**. Schematic representation of the functional domains of EBP50. The GYGF core-binding sequences in PDZ1 and PDZ2 were mutated to GAGA in the S1 and S2 mutants. ΔERM is a truncated form (EBP50-(1-326)) lacking the C-terminal ERM domain. **C.** CHO cells were transiently transfected with empty vector (V), wild-type EBP50 (WT), or EBP50

harboring mutations in the PDZ1 or PDZ2 domains (S1 and S2, respectively) along with GFP-EGFR. Cell lysates were immunoprecipitated with anti-GFP antibody probed for EGFR and EBP50. The interaction between EBP50 and EGFR is lost in the S2 mutant. **D**. CHO cells were transiently transfected with empty vector (V), wild-type EBP50 (WT), or EBP50 harboring mutations in the PDZ1 domain (S1), PDZ2 domain (S2), both PDZ1 and PDZ2 domains (S1/S2) or lacking the C-terminal ERM domain (ΔERM). Cell lysates were immunoprecipitated with anti-FAK antibody and probed for EBP50. The interaction between EBP50 and FAK is lost in the ΔERM mutant.

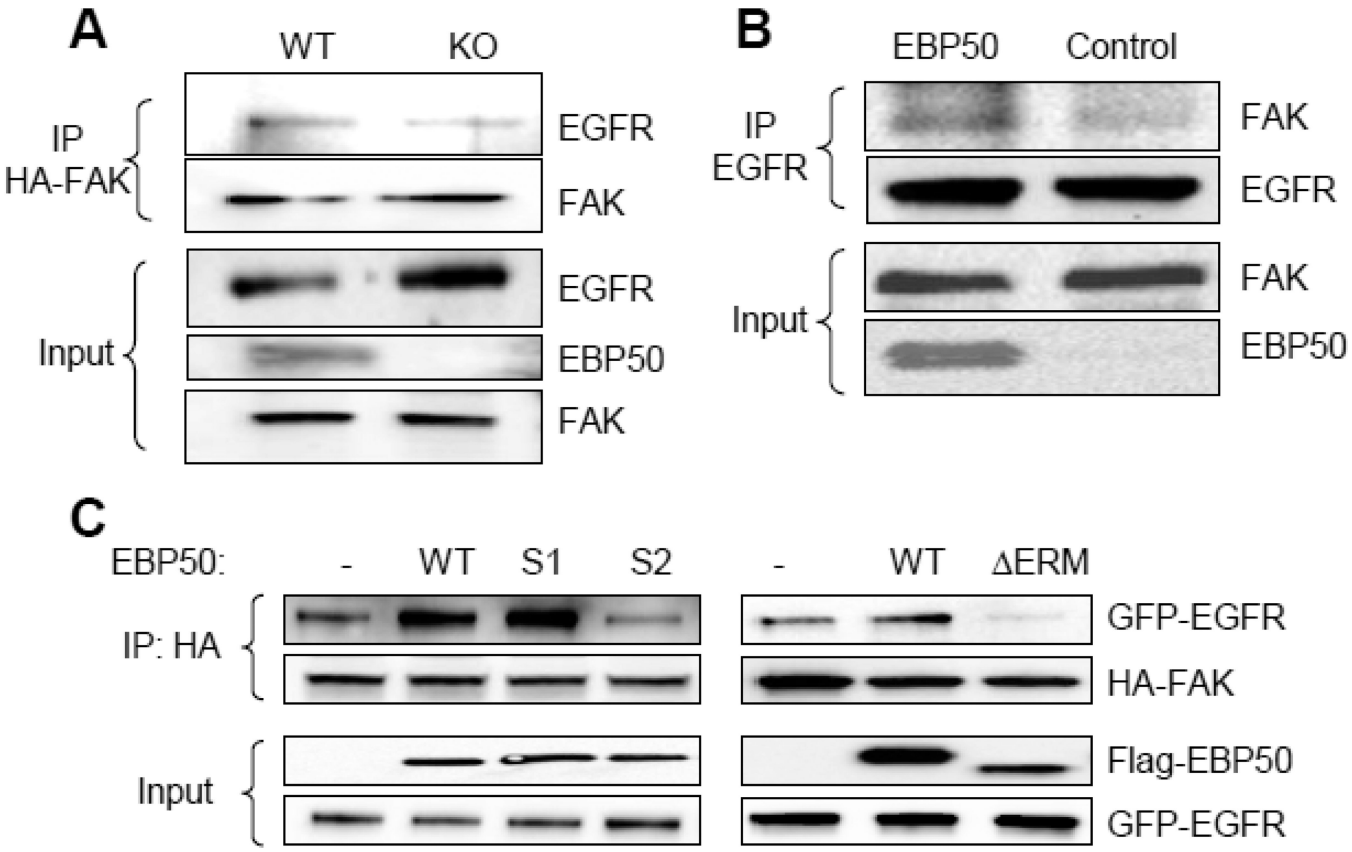

Figure 6. EBP50 assembles FAK and EGFR

A. Primary WT and KO VSMC were electroporated with HA-tagged FAK and GFP-tagged EGFR. Cell lysates were immunoprecipitated with anti-HA antibody. The immunoprecipitate (IP) and lysates (input) were immunoblotted with anti-FAK, anti-EGFR or anti-EBP50, as indicated. **B.** CHO cells were transfected Flag-EBP50 or control empty vector and GFP-EGFR. Cell lysates were immunoprecipitated with anti-GFP antibody. The immunoprecipitate (IP) and lysates (input) were immunoblotted with anti-FAK, anti-EGFR or anti-EBP50, as indicated. EBP50 over-expression increases the interaction between EGFR and FAK. **C**. CHO cells stably expressing GFP-EGFR were transiently transfected with HA-FAK and either empty vector (V), or wild-type (WT), S1, S2 or ΔERM EBP50. Cell lysates were immunoprecipitated with anti-HA antibody and probed for FAK, EGFR and EBP50 as indicated.

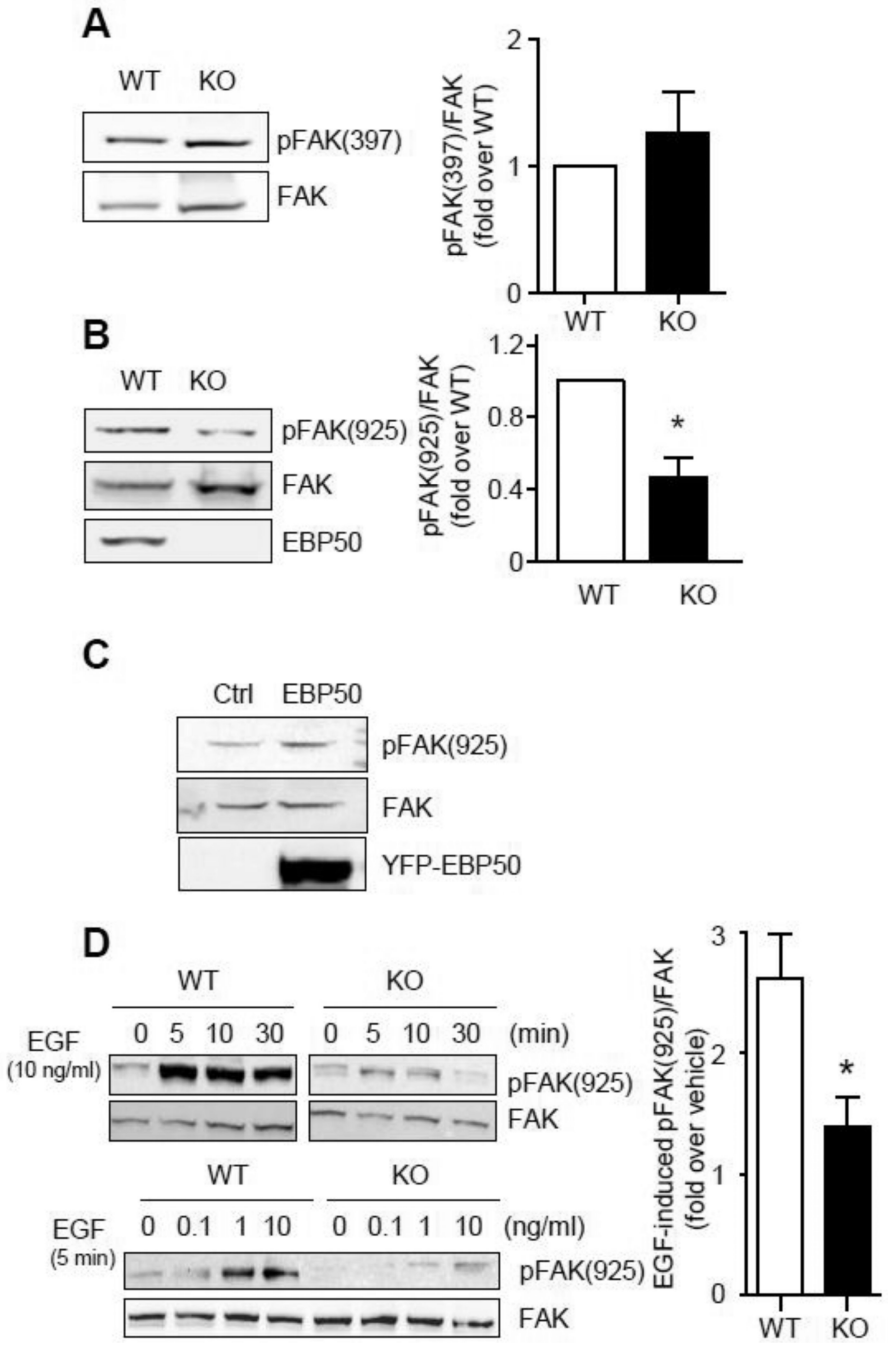

Figure 7. EBP50 increases FAK phosphorylation

Cell lysates from WT and KO VSMC cultured in DMEM containing 10% FBS were analyzed by immunoblotting for phospho-FAK(Tyr-397) (**A**) and phospho-FAK(Tyr-925) (**B**). Graphs shows the average phospho-FAK/total FAK from four independent experiments. *, $p<0.05$. **C**. VSMC were electroporated with empty pcDNA3 (Ctl) or YFP-EBP50, as indicated. Total cell lysates were analyzed by immunoblotting with total and anti-phospho-FAK(Tyr-925) and EBP50. **D**. Upper panels. Serum-starved WT and KO cells were treated with EGF (10 ng/ml) for the indicated times. Lower panels. Serum-starved WT and KO cells were treated with EGF at the indicated concentrations for 5 min. Cells lysates

were subjected to SDS-PAGE and blotted for total and phospho-FAK(Tyr-925). Graph shows the average ratio FAK(Tyr-925) over total FAK from four independent experiments. *, $p<0.05$.

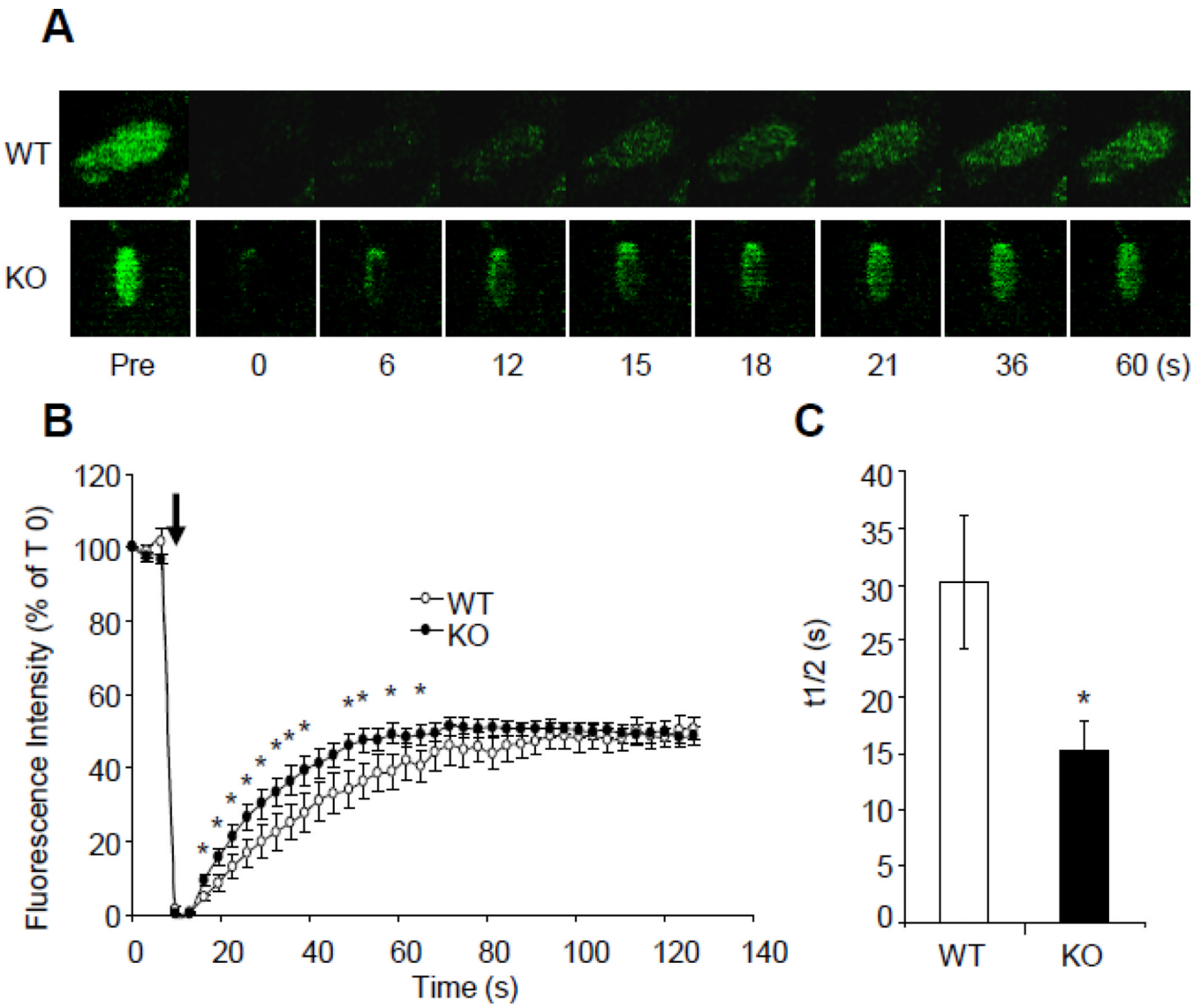

Figure 8. FAK dynamics in WT and KO cells by FRAP

A. Time laps images of single FAs from WT and KO VSMC expressing GFP-FAK in the presence of 10 ng/ml EGF, before bleaching (Pre) and at the indicated times after photobleaching. **B**. Kinetics of fluorescence recovery for GFP-FAK in WT (N=10 FAs) and KO (N=12 FAs) cells. *, $p<0.05$, N=10. **C**. Recovery half-times for GFP-FAK in WT and KO WT cells calculated from the experiments shown in B. *, $p<0.03$.